

Photovoltaic Warm Façades with Phase Change Materials in European Climates

Christian Popp¹, Dirk Weiß², Katja Tribulowski², Bernhard Weller¹

* Corresponding author

¹ Technische Universität Dresden, Institute of Building Construction, Dresden, Germany, christian.popp1@tu-dresden.de

² Technische Universität Dresden, Institute of Building Climatology, Dresden, Germany

Abstract

Since façade-integrated photovoltaic (PV) modules heat up greatly, which reduces the efficiency of the PV, façade panels with PV and phase change materials (PCM) were developed. PCMs absorb a significant amount of thermal energy during the phase transition from solid to liquid, while maintaining a specific melting temperature. This cools down the PV and increases the electrical yield. Numerical studies on PV-PCM warm façades without rear-ventilation have so far been missing. Therefore, a thermal and an electrical simulation model for PV-PCM warm façades were developed and validated. They were then used to analyse the yield increase of two PCM-types and -quantities in PV warm façades facing east, south, and west in Athens, Potsdam, and Helsinki. An annual yield increase of 1.2% to 8.5% for monocrystalline PV modules was determined. The maximum monthly yield increase is 8.0% in Helsinki, 11.4% in Potsdam, and 11.3% in Athens. The study shows that a case-specific selection of the appropriate type and quantity of PCM is necessary. Using the models, a design tool for PV-PCM warm façades will be developed. It will be validated with real monitoring data from PV-PCM façade test rigs at the Technische Universität Dresden and the National Technical University of Athens.

Keywords

Building-integrated photovoltaics, efficiency increase, phase change materials, thermal simulation, yield simulation

10.7480/jfde.2021.1.5513

1 INTRODUCTION

1.1 PHOTOVOLTAIC FAÇADES

As buildings account for nearly 40% of the total energy consumption in Europe, new buildings built from 2021 onwards need to be nearly-zero energy buildings (NZEBs) within the European Union. These NZEBs are energy efficient buildings sourcing locally renewable energies to reduce the energy consumption of the existing building stock (European Commission, 2016).

Building-integrated photovoltaic (BIPV) is an excellent method to achieve this, as it provides renewable energy on-site. Fath (2018) determined a theoretical photovoltaic (PV) potential of 37,700 km² of usable building surfaces with sufficient irradiation for BIPV applications for 2015 in Germany – 65% (24,505 km²) of these areas are façade surfaces. Considering the irradiation, current PV technologies, and plant efficiencies, a theoretical electrical potential of 2,923 TWh can be generated with the whole BIPV potential; 44% (1,286 TWh) of this can be generated through façade applications (Fath, 2018). This theoretically available PV façade potential would be enough to feed the total electricity demand of Germany in 2019, which amounts to 575 TWh (Wilke, 2020), twice. However, the actual number of BIPV applications in façades these days is still low. In 2017, the share of BIPV applications in the total number of PV installations in Europe was estimated to be 2% (Ulrich, 2018).

This low proportion is probably due to some of the disadvantages of using PV on façades. In addition to the lower irradiation compared to inclined PV modules, possible shading situations, and higher reflection losses, the thermal coupling to the building is a decisive factor that must be taken into account when planning façade integrated PV systems (Decker, Grimmig, Mencke & Stellbogen, 1998). Regarding the thermal coupling to the building, one can differentiate between *warm façades* and *cold façades*, which differ in the location and thermal coupling of their outermost layer of the façade (Engin et al., 2016). Accordingly, rear-ventilated façades or double skin façades are called *cold façades*, since the façade cladding is ventilated and thermally decoupled. Wall constructions with thermal insulation composite systems, mullion-transom, or unitized façades are considered *warm façades*, since the façade cladding is in contact with the “warm” interior of the building (Engin et al., 2016; Krippner et al., 2016).

According to Weller, Hemmerle, Jakubetz, and Unnewehr (2009), freely mounted PV modules heat up to 22 K above the ambient temperature. Due to the temperature-dependent performance decrease of photovoltaics, the annual yield of these systems is decreased by 2.0% compared to a PV system running permanently under optimal conditions. For good ventilated *cold façades* temperatures of up to 35 K above the ambient temperature are reached, whereby the annual electrical yield is decreased by 6.0%. The constructional integration of PV modules into the opaque areas of *warm façades* like mullion-transom or unitized façades leads to module temperatures of up to 55 K above the ambient temperature due to missing rear-ventilation. These high temperatures lead to a reduction of the annual electrical yield by 10.5%. Because of this, PV integration into mullion-transom or unitized façades is usually considered unfavourable, even though it comes with constructional benefits: The glasses are supported on all sides linearly, the junction box and cables are hidden in the construction, and regular grid dimensions of mullion-transom façades can lead to more cost-efficiency by series production of the PV façade panels (Weller et al., 2009).

1.2 PHOTOVOLTAIC FAÇADES WITH PHASE CHANGE MATERIALS

One way to reduce the temperature of PV in façades and to increase the electrical yield is to combine the PV modules with phase change materials (PCM). The PCMs absorb a lot of energy during the phase transition from solid to liquid while maintaining their melting temperature and thereby keeping the PV cool and the electrical efficiency high. When the environment cools down and the PCM reaches the freezing temperature, it solidifies and recrystallizes again while transferring the thermal energy to the environment (Horn, Seeger, Scheuring & Weller, 2017).

The integration of PV and PCM in the façade is not a novelty. Giuseppina, Brano, Cellura, Franzitta, and Milone (2012); and Huang, Eames, and Norton (2004) analysed the combination of PV and PCM and developed thermal numerical models, which were validated through comparison with experiments. These models provided the possibility to reproduce the melting process and the thermodynamic behaviour of PCMs. A 1D transient model based on the enthalpy method is presented and validated by Elarga, Goia, and Benini (2017) to analyse the thermal behaviour of a ventilated PV-PCM double skin façade. Depending on the ventilation strategy in the double skin façade, it showed a positive effect of the PCM on the cooling and heating loads. Other similar façade constructions with rear-ventilated PV-PCM systems are analysed numerically and with experimental studies. Aelenei, Pereira, Gonçalves, and Athienitis (2014) combined a PV module with a PCM gypsum board and a ventilation gap between both components to pre-heat the air for space heating. Čurpek and Cekon (2020) analysed a similar system, in which aluminium PCM containers are attached to the rear side of the PV modules and the ventilation gap follows after the PCM containers. Wieprzkowicz, Knera and Heim (2015) presented a numerical study on four organic PCMs in a system with an identical ventilation situation but the PCMs are encapsulated in aluminium honeycomb structures. They concluded that dynamic climate data, location, and orientation of the PV-PCM system are decisive for the right choice of the specific melting temperature and thereby for the choice of a specific type of PCM. Čurpek and Cekon (2020) also point out that there are still difficulties in choosing the right type of PCM depending on the location.

The main research interest focuses on rear-ventilated PV-PCM façades (*cold façades*), which use PCMs both to condition the air for heating buildings and to increase the PV yield. For one of these systems, Wieprzkowicz et al. (2015) determine an average annual PV yield increase of 0.25% by the PCM. The reason for this low yield increase could be the already favourable temperature conditions of PV in rear-ventilated systems, as mentioned in section 1.1. A greater effect of the PCMs and a higher yield increase can be achieved by adding PCM in PV *warm façades*. Here, the basic system reaches higher temperatures, which reduces the annual electrical yield by 10.5% (Weller et al., 2009). These bigger losses provide more potential to be compensated by the PCM. A mullion-transom façade system combining PV modules with encapsulated PCM was developed and monitored by Horn et al. (2017). The monitoring from March to October showed an efficiency increase of 3.4% for thin-film cadmium telluride (CdTe) PV modules. For crystalline PV modules the increase is expected twice as high. Further studies on the influence of PCMs on the PV yield increase of *warm façades* and more information about the location-specific selection of the right type and quantity of PCM are missing. New findings could help to enhance the number of PV façade applications.

This paper addresses the achievable yield increase and its façade-specific influencing factors of PV-PCM *warm façades* without ventilation. PCM capsules are mounted on the rear side of the PV modules, followed by insulation. In this paper, a dynamic thermal simulation model and a PV yield simulation model are presented to analyse the temperature behaviour and the electrical yield of these PV-PCM *warm façades*.

The models are validated and used for a study on the efficiency increase of two types of PCMs in PV-PCM *warm façades*. Different European climates, different façade orientations, and two different PCM quantities are analysed.

2 METHODS

2.1 PCM MATERIAL MODEL FOR THERMAL SIMULATION SOFTWARE

Different PCMs vary in their melting points. Fig. 1 shows the increase of enthalpy of four PCMs, melting at 31 °C (SP31), 26 °C (SP26E), 21 °C (SP21EK) and 15 °C (SP15) on the left. On the right monitoring results from a recently installed PV-PCM test rig at *Technische Universität Dresden (TU Dresden)* are shown. The effect of two different PCMs, SP26EK and SP31 (melting at 26 °C resp. 31 °C), on the temperature of the PV modules is visible. The melting point of the PCMs defines the temperature stage where the enthalpy increases and the cooling is usable.

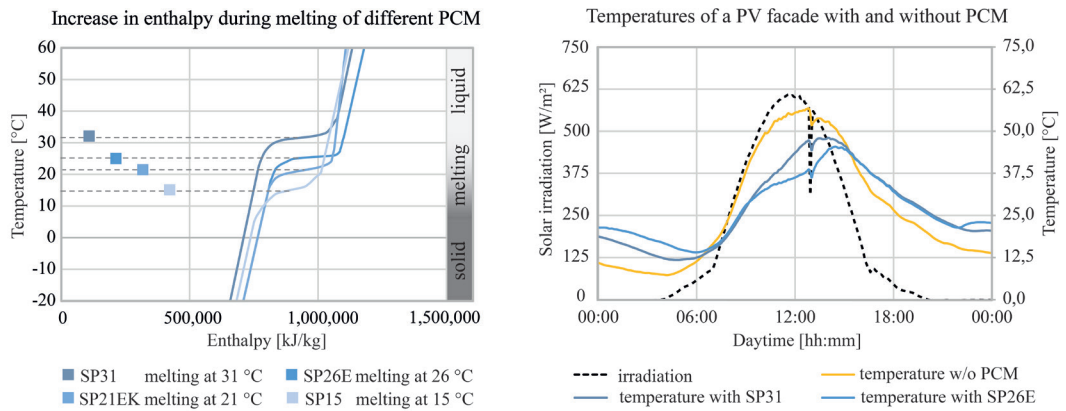


FIG. 1 Increase of enthalpy during melting of different PCMs (left) and the cooling effect of this enthalpy increase on the temperatures of a PV façade system, monitored at a test rig at TU Dresden (right).

To analyse the thermal behaviour of PCMs, a dynamic enthalpy model for the integration into the thermal simulation software *DELPHIN* was developed. The model works with the following basic assumptions and physical equations:

- The change in the internal energy of a body is proportional to the change in temperature and to the mass of the body, which usually remains constant. It is described by the specific heat capacity c_p [$J/(kg \cdot K)$].
- The internal energy U depends on the mass m , the specific heat capacity c_p and the temperature T . It is described with the equation (1):

$$U = m \cdot c_p \cdot T \quad (1)$$

- The change of the internal energy by change of temperature is described with the equation (2):

$$\Delta U = m \cdot c_p \cdot \Delta T \quad (2)$$

- In order to change the state of aggregation, energy must be added or withdrawn. The energy required for this depends on the material (specific melting/boiling energy E_m or E_b [kJ/kg]) and the mass of the body.
- The change in internal energy that is required for a change in the state of aggregation is described by (3):

$$\Delta U_{phase\ change} = m \cdot E_{m/b} \quad (3)$$

- This must be added to the internal energy if a change of the state of aggregation has occurred (4):

$$U = m \cdot c_p \cdot \Delta T + \Delta U_{phase\ change} \quad (4)$$

In order to model the abrupt change of the internal energy during the transition of the state of aggregation of PCMs, the function of the specific heat capacity of a standard material was virtually changed. An offset for the phase change was implemented in the function, which normally depends linearly on the temperature. This offset reproduces the change in the internal energy of the PCMs during melting resp. solidification, as shown in Fig. 1 (left). To create this function, the thermal characteristics given on the PCM data sheets of the suppliers are fed into the PCM material model. The course of the internal energy of the PCMs is determined gradually. According to equation (1) the inner energy at absolute zero point is zero. From this point on, the course of the internal energy is calculated for the different states of aggregation, with their temperature-specific material parameters. The internal energy of the preceding temperature stages is increased by the internal energy of the following temperature stages (5):

$$U_{(n+1)} = m \cdot c_{p,n+1} \cdot (T_{(n+1)} - T_{(n)}) + U_n \quad (5)$$

Besides typical material parameters, like density, specific heat capacity, and thermal conductivity, the function for the thermal storage behaviour is implemented in a material file of the thermal simulation software. The function replaces the generally given material parameters during the transition of the state of aggregation. Thus, the enthalpy function as shown in Fig. 1 (left) is reproduced in the model.

2.2 ELECTRICAL YIELD CALCULATION

The electrical yield calculation is based on the one-diode model. To model the dynamic relationship between the current and voltage of PV modules, the voltage-current characteristic curve needs to be determined. The manufacturer's data sheets provide three points on this characteristic curve (short-circuit current, open-circuit voltage and maximum power point). A system of equations, according to Dobos (2012), is used to determine the missing parameters for calculating the dynamic values of current and voltage. The dynamic current-voltage curve can then be fully mapped and the electrical PV power can be calculated for each time step, depending on temperature and irradiation (Dobos, 2012; Hansen, 2015).

The module temperature and the irradiation on the surface of the PV module are determined using the thermal simulation software, which uses data from climate files (e.g. epw-files).

3 STUDY ON PV-PCM WARM FAÇADES IN EUROPEAN CLIMATES

3.1 METHODOLOGY

To analyse the effect of different PCMs and their quantities on the electrical output of differently located and oriented PV *warm façades*, the developed PCM material model, the thermal simulation software *DELPHIN*, and the one-diode model were used. Fig. 2 (left) shows the main components of the PV-PCM *warm façade* and the simplified simulation model. The capsule contains fins for higher thermal contact surface to the PCM. The mullion resp. transom is not modelled, as prior studies determined its influence on the results is less than 0.5% and in doing so, the simulation time was reduced significantly. The electrical yield calculations consider a PV module with 60 cells of monocrystalline silicon (also Solar SL19 270). The material data of the analysed PCMs is shown in Table 1.

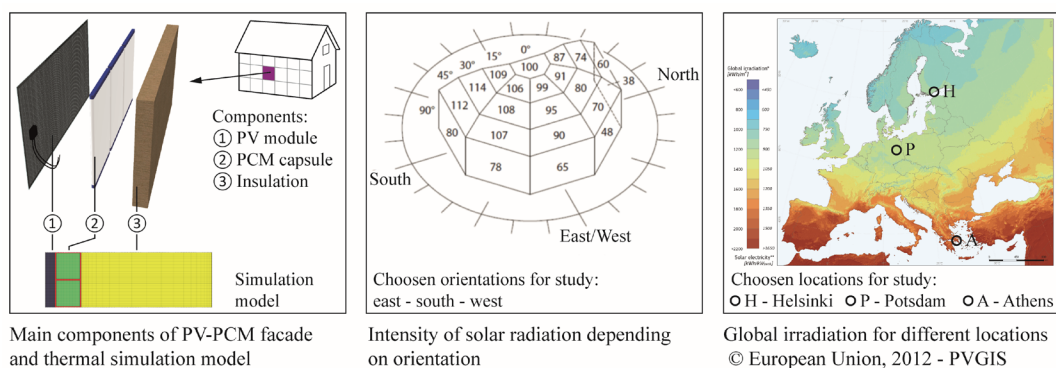


FIG. 2 Schematic layout of the PV-PCM façade and influence of the orientation and location on the solar irradiation

The proper functionality of all three models was tested first. The thermal simulation and the material model were compared to real test results. For the electrical tool, a comparison to a commercial PV planning software (*PV*SOL*) was carried out. In a second step, yield simulations with long-term average climate data were carried out for two types of PCM (SP21EK and SP31 from the company *Rubitherm GmbH*) in east-, south-, and west-facing PV-PCM *warm façades* for Helsinki, Potsdam, and Athens, as shown in Fig. 2 (centre and right). The thickness of the PCM capsules was increased from 10 mm to 20 mm in a third step for both PCMs and all orientations and locations.

TABLE 1 PCM parameters of the simulations

PCM	SP21EK	SP31	
melting range	22 - 23	31 - 33	[°C]
density	1,3 - 1,35	1,4 - 1,5	[kg/l]
thermal conductivity	~ 0,5	~0,5	[W/(m K)]
specific heat storage capacity	2	2	[kJ/(kg K)]
heat storage capacity during phase change	170 (at 13 °C to 28 °C)	210 (at 23 °C to 38 °C)	[kJ/kg]
thickness PCM	10, 20	10, 20	[mm]

3.2 VALIDATION OF THERMAL SIMULATION MODEL

First, a simulation model of a PV mullion-transom façade without PCM was developed and compared to real monitoring values from a PV façade without PCM at a test rig at TU Dresden. In the simulation model, the real climate data gathered from the monitoring were implemented. Fig. 3 shows the temperature curves of the simulation and the monitoring for January, May, and August. The comparison of the temperature curves shows a good correspondence, especially in the months with high irradiation (spring to summer). The higher deviations in January are probably caused by the albedo. This was assumed constantly at 0.2 in the simulation, but is variable in reality and can increase to values of 0.8 in case of snow. The total annual average deviation between simulation and monitoring is 2.66 K. This is considered to be sufficiently low for further analyses.

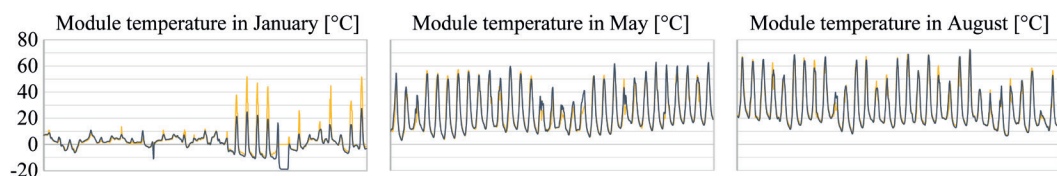


FIG. 3 Temperature curves of simulation and monitoring for January, May, and August

3.3 VALIDATION OF THE PCM MATERIAL MODEL

For the validation of the PCM material model, a quality test from production control of the PCM supplier and developer was simulated. During this *three-layer calorimeter test*, a chilled PCM sample is put into an insulated box, which is placed in a heat cabinet. The heat cabinet runs a temperature curve depending on the melting point of the PCM. The temperature in the middle of the

PCM sample is recorded. Fig. 4 shows the setup of the test schematically (left) and proves that the simulation model can reproduce the temperature curve of the real test properly (right). The short-term “sub cooling” of the PCM, which is indicated by a local minimum before solidification, after approximately 1000 minutes at SP21EK and 1600 minutes at SP31, is not reproduced by the PCM model. The reason for this is found in an asymmetry between the melting and the solidification process of PCMs in reality. This hysteresis is not implemented in the model, because the model assumes a symmetrical course for the melting and the solidification process. However, the relevant melting process, which happens when the solar energy is converted into electricity by the PV, is reproduced properly. Therefore, the PCM material models are considered sufficiently accurate for the analysis of the PV yield.

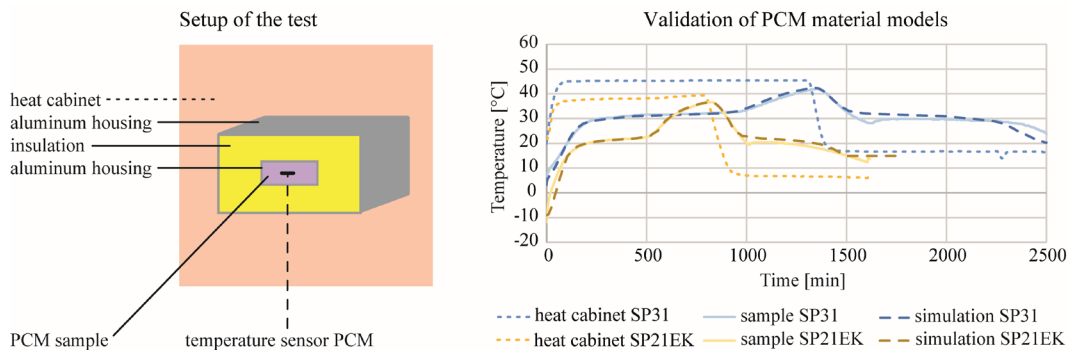


FIG. 4 Schematic sketch of production control test (left) and temperature curves of simulation and real tests for validation of PCM material models of SP31 and SP21EK (right)

3.4 VERIFICATION OF THE ELECTRICAL YIELD CALCULATION TOOL

The electrical yield calculation (hereafter called “PV-Tool”) was verified by comparing it to commercial state-of-the-art PV planning software. The input parameters, boundary conditions, and analysed systems were identical. To cover different environmental influences, the simulations were carried out for monocrystalline PV systems in *warm façades* without PCM in Helsinki, Potsdam, and Athens, each with east, south, and west orientations. Fig. 5 shows the monthly deviation (left) and the total annual deviation (right) between the PV-Tool and the commercial software for all locations and orientations. During the months with high irradiation (April to October), the simulations show a good match with low deviations between -7% to +9%. The maximum deviation within one single month appears in Helsinki in December with -25%. For Potsdam and Helsinki, the maximum deviation is in the winter months, when the irradiation is low. Over the whole year, only small deviations between the simulations exist. The deviations are below 1% in Potsdam, below 2% in Helsinki, and below 4% in Athens.

A validation based on real measured data will help to better evaluate the accuracy of the electrical yield calculation model. A sensitivity analysis with focus on situations with low radiation, a high percentage of diffuse radiation, and high reflections can help to make an assessment of possible weak points.

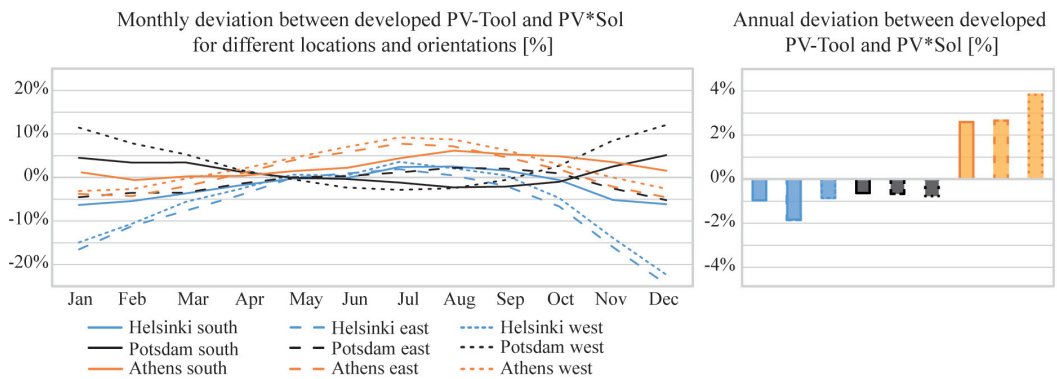


FIG. 5 Monthly (left) and total (right) deviation between electrical yield calculation model and PV planning software

3.5 ELECTRICAL YIELD HELSINKI

Helsinki is located at 60 degrees latitude and reaches a maximum sun elevation angle of 53.3° in summer. This means that the reflection losses are low in summer and only visible in the results of the south façade in June. All orientations have their yield maximum and the maximum efficiency increase by the PCMs in summer. At this time of the year, the south façade in Helsinki reaches higher yields than the façades in Potsdam and Athens. In the winter months, the yield is barely increased because the melting temperature of the PCMs investigated is rarely reached. Overall, the annual yield on the east and south façade is comparable to that of Potsdam. Fig. 6 shows the electrical output and its increase through the analysed PCMs in 10 mm and 20 mm thick capsules for east, south, and west façades.

The yield increase of the PCMs reaches a minimum of 0.1% with 10 mm of SP31 in December on the east façade and a maximum of 8.0% with 20 mm of SP21EK in August on the south façade. From November to February, the two PCMs achieve additional yields over 1.0% only on the south façade. On the west façade, this is only possible with 20 mm of SP21EK. All other variants show low additional yields below 1.0% in this time. The average additional yield between November and February for 20 mm of SP21EK is 0.7% (east), 2.6% (south), and 1.1% (west). In these variants, 20 mm of SP31 achieve 0.5% (east), 1.8% (south), and 0.9% (west). During the period of high irradiation, from March to October, the SP21EK in 20 mm capsules achieves additional yields of 3.5% (east), 6.6% (south), and 4.7% (west), while the SP31 produces 1.7% (east), 3.8% (south), and 2.7% (west).

Thus, depending on the orientation, the SP31 achieves about half of the yield increase in summer and about one fifth to one third of the yield increase in winter, compared to the SP21EK. It is also found that the 10 mm of SP21EK achieves a higher annual yield than the doubled quantity of 20 mm of SP31 at all orientations. Due to the lower melting point of the SP21EK, the cooling effect starts earlier, in all orientations in the summer months. Doubling the PCM capsule thickness to 20 mm leads to a further yield increase from 33% to 51%, depending on the orientation of the façades. A PCM with a melting point below SP21EK or between SP21EK and SP31 might achieve a higher increase. Since the albedo was constant during the simulation, higher irradiation values on the façade could occur in reality in winter. As a result, the PV output in winter and its increase due to the PCM could also be slightly higher.

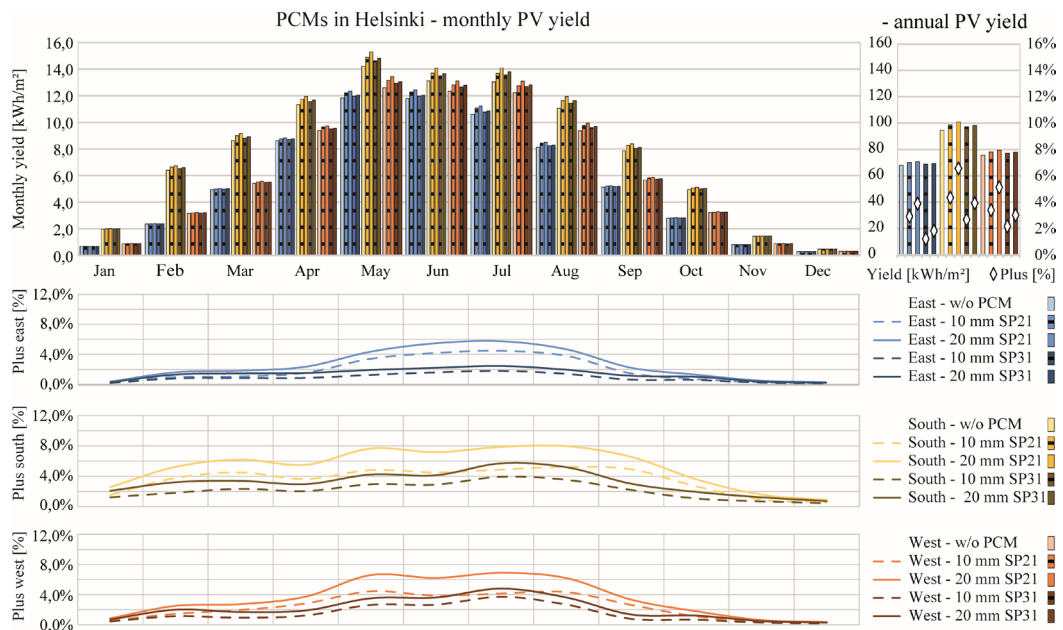


FIG. 6 Monthly electrical output of a PV warm façade without and with PCM in Helsinki (top - left), absolute and relative annual PV yield (top - right) and monthly yield increase for all three orientations and both PCMs (bottom)

3.6 ELECTRICAL YIELD POTSDAM

Potsdam is located at 52 degrees latitude and reaches a maximum sun elevation angle of 62.0° in summer. This results in higher reflection losses on the south façade in summer compared to Helsinki. The east and west façades are not affected by this and reach their maximum in summer. The minimum yield increase by the PCMs in Potsdam is 0.3% with 10 mm of SP31 in east orientation in December. A maximum increase of 11.4% is reached with 20 mm of SP21EK in September on the west façade. Fig. 7 shows the results for the analysed PCMs, capsule dimensions, and orientations.

With both PCMs, an efficiency increase is possible even in the winter months. The average additional yield between November and February for 20 mm of SP21EK is 1.0% (east), 5.6% (south) and 3.0% (west). For these variants, 20 mm of SP31 achieve 0.8% (east), 3.6% (south), and 2.2% (west). During the time with higher irradiation, from March to October, the SP21EK in 20 mm capsules achieves additional yields of 4.4% (east), 8.7% (south), and 9.1% (west), while the SP31 gains 2.5% (east), 6.0% (south), and 7.6% (west) extra yield in this period.

Thus, depending on the orientation, the SP31 in Potsdam achieves 17% to 43% less efficiency increase in summer and 20% to 35% less efficiency increase in winter than the SP21EK. Only on the west façade in June, July, and August, the yield increase of the SP31 is, at 6%, slightly higher than that of the SP21EK. As the SP21EK melts earlier than the SP31 during the course of a day in summer, less cooling potential is available when the sun shines on the west façade in the afternoon. Nevertheless, all variants show that the SP21EK achieves a significantly higher annual yield increase than the SP31. Again, the melting point at 21 °C, and thus the cooling effect of the SP21EK, can be used more often throughout the year. On the east façade, the annual yield of 10 mm of SP21EK is higher than the yield of the doubled amount of 20 mm of SP31. On the south façade, 10 mm of SP21EK and 20 mm of SP31 reach almost the same yield. Only on the west façade, the 20 mm of SP31 produces significantly more yield than 10 mm of SP21EK. In Potsdam, a doubling of the

PCM capsule from 10 mm to 20 mm leads to a further yield increase of 26% to 63% depending on the façade orientation. PCMs with a melting point between the two PCMs could be analysed for further potential.

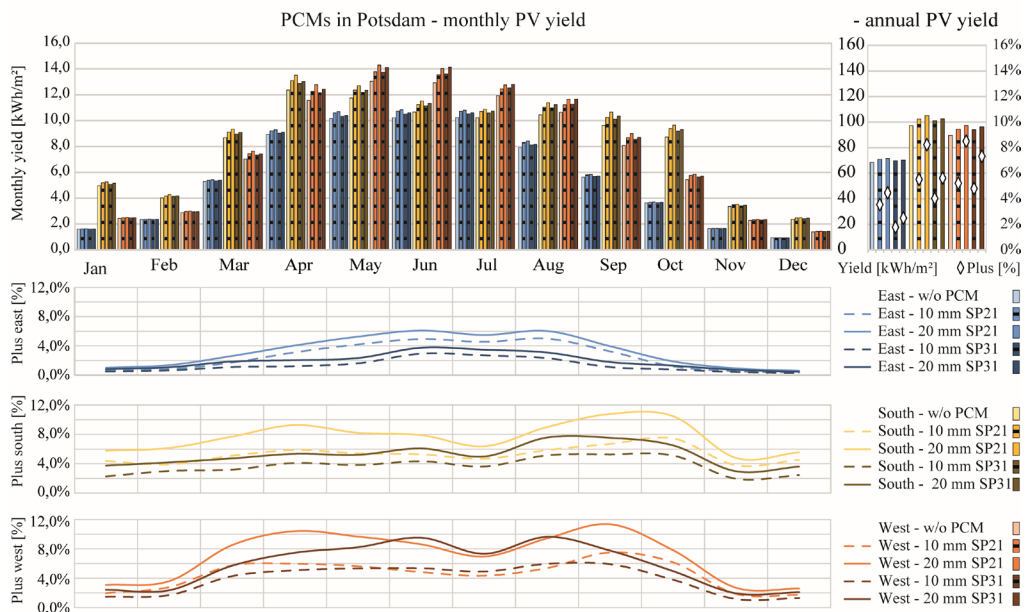


FIG. 7 Monthly electrical output of a PV warm façade without and with PCM in Potsdam (top - left), absolute and relative annual PV yield (top - right), and monthly yield increase for all three orientations and both PCMs (bottom)

3.7 ELECTRICAL YIELD ATHENS

Athens is located at 37 degrees latitude and reaches a sun elevation angle of 45° as early as March. The angle increases to a maximum sun elevation angle of 75.5° in June. As early as April, yield losses due to reflection losses on the south façade become apparent, which continue until August. The east and west façades reach their typical maximum in summer. Fig. 8 shows the output and its increase in Athens for the analysed PCMs, capsule dimensions, and orientations.

Both PCMs generate additional yields throughout the year. The lowest efficiency increase of the PCM in Athens is 0.9% with 10 mm of SP31 in the east orientation in December, while the maximum efficiency increase of 11.3% is achieved with 20 mm of SP31 in September on the south façade. The additional yield of 20 mm SP21EK from October to May averages at 5.1% (east), 9.6% (south), and 6.8% (west) and is higher than for 20 mm of SP31 with 2.7% (east), 6.6% (south), and 4.4% (west). Depending on the orientation, the SP31 thus achieves 31% to 47% less efficiency increase than the SP21EK in these months. From June to September, however, the SP31 is more productive in all façade orientations. Here, 20 mm of SP21EK achieves an average yield increase of 4.7% (east), 4.1% (south), and 4.4% (west) and 20 mm of SP31 achieves 8.2% (east), 8.9% (south), and 10.2% (west). This means that the SP21EK achieves 43% to 57% less yield increase than the SP31 in these months. In the summer months, temperatures in Athens are so high that the SP21EK melts too early in the course of the day or cannot recrystallize completely during night. Therefore, SP21EK in summer in Athens only reaches a lower cooling and a lower additional output. This can be

seen in all façade orientations between May and October. A similar phenomenon can be observed with 10 mm SP31, especially in the south and west orientation. Doubling the quantity of SP31 to 20 mm helps to reach sufficient enthalpy capacity to achieve a significantly higher efficiency increase between May and September.

For Athens, it can be concluded from the results that SP21EK and SP31 lead to comparable efficiency increase. On the east and south façades, the additional yield of SP21EK in the cooler phase of the year is equal to the additional yield of SP31 in the warmer phase of the year. On the west façade, SP31 has a significant increase in additional yield of 0.9 (for 10 mm) and 1.4 (for 20 mm) percentage points compared to SP21. Doubling the PCM capsule thickness leads to a further yield increase of 32% to 61% in Athens, depending on the orientation. Further potential can probably be achieved by a PCM with a melting point somewhere between the two PCMs investigated.

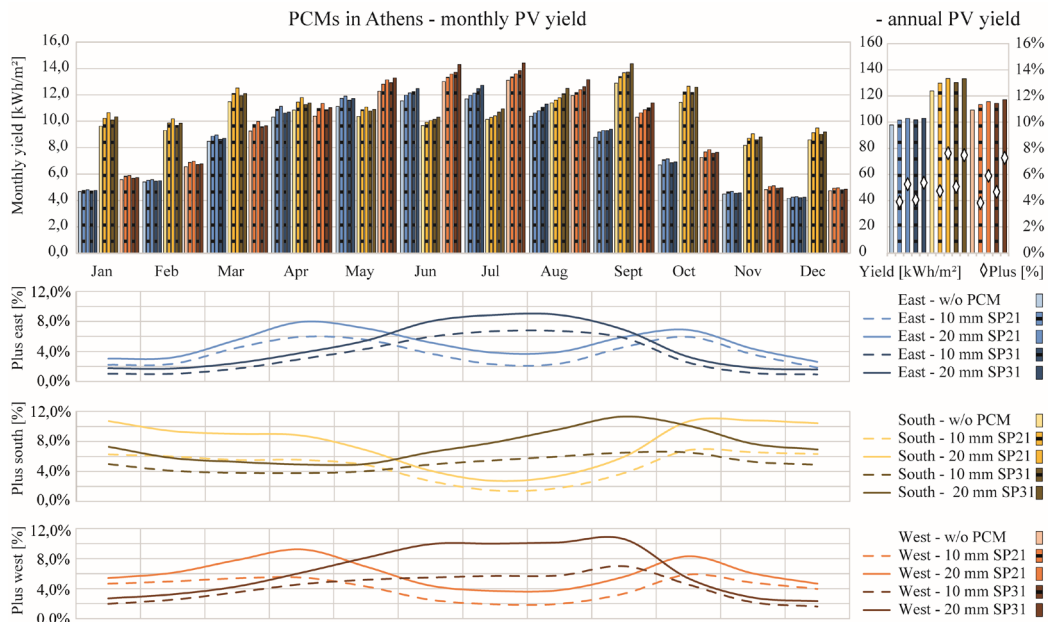


FIG. 8 Monthly electrical output of a PV warm façade without and with PCM in Athens (top - left), absolute and relative annual PV yield (top - right), and monthly yield increase for all three orientations and both PCMs (bottom).

4 DISCUSSION

The study shows that the combination of the analysed PCMs and monocrystalline PV modules in east-, south-, and west-oriented façades in Helsinki, Potsdam, and Athens leads to an annual yield increase of 1.2% to 8.5%. In the moderate climates (Helsinki and Potsdam), SP21EK proved to be more productive. In Helsinki, the SP21EK performed better than the SP31, regardless of the orientation of the façade. All year round, the most productive combination is 20 mm of the SP21EK on the south façade, achieving a yield increase of 6.6%. In Potsdam, the SP21EK is more productive than the SP31 and reaches a maximum annual yield increase of 8.5% with 20 mm capsules on the west façade. In the Mediterranean climate, the higher melting point of SP31 achieves comparable or even higher results than the SP21EK. In Athens, it was found that the optimal type of PCM changes over the course of the year and depends on the orientation and quantity of PCM. Throughout the

year, 20 mm of SP21EK achieves the highest additional yield of 7.6% on the south façade. At 7.5%, 20 mm of SP31 reaches almost the same amount in this orientation. The SP21EK achieves the highest increase in spring and autumn while the SP31 is more productive in summer. Utilising this, it becomes possible to selectively support the yield increase in a certain phase of the year, when the electricity demand is higher (e.g. spring and autumn).

For all orientations in Helsinki and for the east and south orientations in Potsdam, it was found that 10 mm of SP21EK reaches higher yields than the double amount (20 mm) of SP31. According to this, by choosing the right PCM, the required quantity can be greatly reduced. Results also show that doubling the quantity of PCM from 10 mm to 20 mm results in a further yield increase between 26% and 63% for the analysed variants. An increase in the quantity of PCM will therefore increase the costs proportionally, but the yield will only increase on a diminishing scale. Since the cost of the PCMs and the reachable additional yield are crucial decision factors for the realisation of PV-PCM *warm façades*, location and orientation dependent dimensioning is necessary. The analysis of further PCMs will also offer additional possibilities for yield increase.

5 CONCLUSION AND PROSPECT

This work focuses on the integration of PCMs in PV *warm façades*. The achievable yield increase of these systems depending on location, orientation, and PCM type and quantity was analysed for the first time. It was shown that PV-PCM *warm façades* achieve a significantly higher average annual PV yield increase (e.g. 8.5% in Potsdam, south oriented), compared to rear-ventilated PV-PCM façades (0.25% (Wieprzkowicz et al., 2015)). This makes the use of PCMs in PV *warm façades* attractive. Simulation models were developed and validated. A numerical study with these models showed that the location and orientation strongly influence the optimal melting range and thus the required PCM type and quantity. Productive PCM melting ranges can be derived for the analysed locations. Melting ranges around 20 °C to 25 °C for Helsinki and Potsdam and 25 °C to 30 °C for Athens seem promising. By adjusting the melting range, the maximal yield increase could also be achieved in spring and autumn to create a more homogeneous energy production over the course of the year.

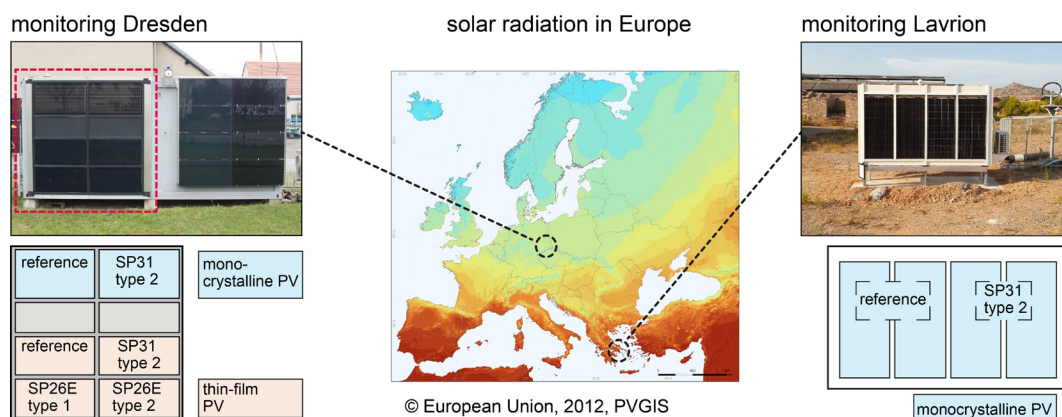


FIG. 9 Monitoring test rigs with PV-PCM warm façades in Dresden and Lavrion for the validation of the PV-PCM design tool

For the effective and economical use of PV-PCM *warm façades*, a case-specific dimensioning is required to reduce the quantity of PCM. For this purpose, a design tool will be developed that can take into account different orientations, locations, PCM types and quantities, PV modules, and insulation thicknesses. The design tool will be based on the simulation models and calculation methods described in this paper. In order to achieve a validation of the whole design tool, free field measurements on PV-PCM façade test rigs will be used. For this purpose, two monitoring test rigs with different PV technologies, different PCM types and capsule types have been installed. One is located at *TU Dresden* and the second on a property of the *School of Mining and Metallurgical Engineering* of the *National Technical University of Athens (NTUA)* in Lavrion, Greece, as shown in Fig. 9.

Acknowledgements

This work originated from the research project PV-Tool – Development of a simulation tool for dimensioning of modular energy producing façade systems with phase change materials, funded within the scope of the Central Innovation Program for SMEs (German: Zentrales Innovationsprogramm Mittelstand, ZIM) of the Federal Ministry of Economic Affairs and Energy (grant number: ZF4123720HF8). The authors are grateful to all project partners for their excellent cooperation. The authors would like to thank Dimitris Mantelis from the NTUA for the excellent and collegial cooperation.

References

- Aelenei, L., Pereira, R., Gonçalves, H., & Athienitis, A. (2014). Thermal Performance of a Hybrid BIPV-PCM: Modeling, Design and Experimental Investigation. *Energy Procedia*, 48. <https://doi.org/10.1016/j.egypro.2014.02.056>.
- Čurpek, J., & Cekon, M. (2020). Climate response of a BiPV façade system enhanced with latent PCM-based thermal energy storage. *Renewable Energy*. <https://doi.org/10.1016/j.renene.2020.01.070>.
- Decker, B., Grimmig, B., Mencke, D., & Stellbogen, D. (1998). Besonderheiten bei der Projektierung von Photovoltaikfassadenanlagen [Special requirements for the planning of photovoltaic façade systems]. *Forschungsverbund Sonnenenergie - "Themen 97/98; Solare Gebäudetechniken*, 95-103.
- Dobos, A. (2012). An Improved Coefficient Calculator for the California Energy Commission 6 Parameter Photovoltaic Module Model. *Journal of Solar Energy Engineering*, 134. <https://doi.org/10.1115/1.4005759>.
- Elarga, H., Goia, F., & Benini, E. (2017). PV-PCM integration in glazed buildings. Numerical study through MATLAB/TRNSYS linked model. *Building Simulation Applications 2017*, 3.
- Engin, B., Brandau, K., Flohr, S., Horn, S., Roos, M., Vaupel, G., & Bernhard, W. (2016). Photovoltaik Fassaden: Leitfaden zur Planung [Photovoltaic façades: planning guide]. *DAW SE und GWT-TUD GmbH*.
- European Commission. (2016). *Commission Recommendation (EU) 2016/1318 - Of 29 July 2016 - On guidelines for the promotion of nearly zero-energy buildings and best practices to ensure that, by 2020, all new buildings are nearly zero-energy buildings*. 12.
- Fath, K. (2018). Technical and economic potential for photovoltaic systems on buildings. (Doctoral dissertation). *KIT Scientific Publishing, Band 25_Produktion und Energie*. <https://doi.org/10.5445/KSP/1000081498>.
- Giuseppina, C., Lo Brano, V., Cellura, M., Franzitta, V., & Milone, D. (2012). A finite difference model of a PV-PCM system. *Energy Procedia*, 30, 198-206. <https://doi.org/10.1016/j.egypro.2012.11.024>.
- Hansen, C. (2015). Parameter Estimation for Single Diode Models of Photovoltaic Modules. *Sandia Report SAND2015-2065*. <https://doi.org/10.13140/RG.2.1.4336.7842>.
- Horn, S., Seeger, J., Scheuring, L., & Weller, B. (2017). Fassade mit temperaturregulierenden Photovoltaik-Paneelen - Ergebnisse aus einem ersten Praxistest [Façade with temperature-regulating photovoltaic panels - results from a first field test]. *ce/papers*, 1(1), 240-253. <https://doi.org/10.1002/cepa.25>.
- Huang, M. J., Eames, P. C., & Norton, B. (2004). Thermal regulation of building-integrated photovoltaics using phase change materials. *International Journal of Heat and Mass Transfer*, 47, 2715-2733. <https://doi.org/10.1016/j.ijheatmasstransfer.2003.11.015>.
- Krippner, P. D. R., Becker, P. D. G., Maslaton, P. D. M., Maurer, D. C., Seltmann, T., Kuhn, T. E., Kämpfen, B., Reinberg, G. W., Haselhuhn, R., & Hemmerle, C. (2016). Gebäudeintegrierte Solartechnik: Photovoltaik und Solarthermie - Schlüsseltechnologien für das zukunftsfähige Bauen: Energieversorgung als Gestaltungsaufgabe [Building-Integrated Solar Technology: Architectural Design with Photovoltaics and Solar Thermal Energy] (1. Edition). *Institut für internationale Architektur-Dokumentation GmbH & Co. KG, DETAIL*.
- Ullrich, S. (2018, October 16). Der Mehrpreis schreckt ab [The additional price deters]. *photovoltaik*, 10-2018, 10-13.
- Weller, B., Hemmerle, C., Jakubetz, S., & Unnewehr, S. (2009). Detail Praxis: Photovoltaik: Technik, Gestaltung, Konstruktion [Photovoltaics: Technology, Architecture, Installation] (1. Edition). *Institut für internationale Architektur-Dokumentation GmbH & Co. KG, DETAIL*.
- Wieprzkowicz, A., Knera, D., & Heim, D. (2015). Effect of Transition Temperature on Efficiency of PV/PCM Panels. *Energy Procedia*, 78, 1684-1689. <https://doi.org/10.1016/j.egypro.2015.11.257>.
- Wilke, S. (2020, March 16). Stromerzeugung erneuerbar und konventionell [Renewable and conventional power generation]. *Umweltbundesamt*. <https://www.umweltbundesamt.de/daten/energie/stromerzeugung-erneuerbar-konventionell>.